



The characteristics of emphysema and pulmonary perfusion derived from spectral CT in smokers

Yu Guan^{#^}, Xiuxiu Zhou^{#^}, Di Zhang, Yi Xia, Shiyuan Liu[^], Li Fan[^]

Department of Radiology, Second Affiliated Hospital of Naval Medical University, Shanghai, China

Contributions: (I) Conception and design: Y Guan, X Zhou, S Liu, L Fan; (II) Administrative support: S Liu, L Fan; (III) Provision of study materials or patients: Y Guan, L Fan; (IV) Collection and assembly of data: Y Guan, X Zhou, Y Xia, S Liu, L Fan; (V) Data analysis and interpretation: All authors; (VI) Manuscript writing: All authors; (VII) Final approval of manuscript: All authors.

[#]These authors contributed equally to this work.

Correspondence to: Shiyuan Liu, MD, PhD; Li Fan, MD, PhD. Department of Radiology, Second Affiliated Hospital of Naval Medical University, No. 415 Fengyang Road, Shanghai 200003, China. Email: radiology_cz@163.com; fanli0930@163.com.

Background: Tobacco smoking may cause pulmonary perfusion abnormality. Assessment of the lung perfusion characteristics is very significant to timely treatment and prevent disease progression in smokers. The purpose was to investigate the value of iodine maps from spectral dual-layer detector computed tomography (DLCT) in assessing lung perfusion changes in smokers.

Methods: Nineteen smokers and 29 non-smokers who underwent dual-phase contrast enhanced scans on a spectral DLCT were retrospectively collected. Emphysema on non-contrast images and perfusion defect (PD) on iodine maps were scored visually at bilateral lung fields of three anatomic levels (on the slice of the aortic arch, the carina, and the aperture of the inferior pulmonary veins). The scores were calculated based on the ratio of the abnormality occupied in the pulmonary field of each slice as described below: point 0, no abnormality; point 1, $0% < \text{abnormality scope} \leq 25%$; points 2, $25% < \text{abnormality scope} \leq 50%$; points 3, $50% < \text{abnormality scope} \leq 75%$; points 4, abnormality scope $> 75%$. The sum of scores for each patient was calculated. The iodine density (ID) of PD and thoracic aorta were measured respectively (ID_{defect} , $ID_{\text{thoracic aorta}}$), then calculating the ratio as the normalized ID (nID). Emphysema index (EI) was defined as the volume percentage of the lung attenuation below -950 Hounsfield units. The percentage of forced expiratory volume in 1 second (FEV_1) to the predicted value ($FEV_1\%$) and the ratio of FEV_1 to forced vital capacity (FVC) were recorded. The differences of the emphysema and PD visual scores, ID_{defect} , nID, EI were analyzed by analysis of variance between smokers and non-smokers. Correlations between emphysema, PD and $FEV_1\%$, FEV_1/FVC were evaluated by Spearman correlation analysis.

Results: The PD visual scores on ID images were significantly higher in smokers compared with that in non-smokers ($P=0.014$), while no significantly difference was found for emphysema visual scores ($P=0.402$). Both ID_{defect} and nID were significantly lower in smokers compared with non-smokers ($P=0.003$; $P=0.029$), while no significantly difference was found for EI ($P=0.061$). Besides, PD visual scores were negatively correlated with $FEV_1\%$ ($r=-0.61$, $P=0.025$) and FEV_1/FVC ($r=-0.62$, $P=0.024$) for smokers.

Conclusions: Compared with emphysema, the iodine map derived from spectral DLCT showed higher sensitivity for the evaluation of the pulmonary abnormalities of smokers.

Keywords: Tobacco smoking; emphysema; lung perfusion; spectral computed tomography

Submitted Jun 11, 2023. Accepted for publication Oct 13, 2023. Published online Nov 17, 2023.

doi: 10.21037/jtd-23-891

View this article at: <https://dx.doi.org/10.21037/jtd-23-891>

[^] ORCID: Yu Guan, 0000-0001-9416-058X; Xiuxiu Zhou, 0000-0003-2405-0566; Shiyuan Liu, 0000-0003-3420-0310; Li Fan, 0000-0003-4722-3933.

Introduction

Tobacco consumption is the primary contributing factor to chronic obstructive pulmonary disease (COPD) across the globe. Far more than 15% of smokers would develop COPD (1). Furthermore, a significant number of smokers without spirometry abnormality might have respiratory symptoms and pulmonary structural abnormalities manifested as the varying presence of emphysema and small airway disease (2,3). These pulmonary structural abnormalities can be found and quantified with computed tomography (CT) (4,5). Abnormal pulmonary blood circulation is also one of the most major pathophysiological alterations in smokers. According to the present research, tobacco smoking is vasoactive and seriously influences the pulmonary vascular structure. Moreover, blood vessel dysfunction contributes to vascular remodeling, pulmonary hypertension (PH) and eventually pulmonary heart disease. Recent studies provide evidence that pulmonary vascular alterations often precede with airflow limitation and alveolar destruction (6,7), and targeting vascular therapy seems to be a promising treatment to cure and prevent disease progression. Therefore, assessment of the lung perfusion abnormality is very significant to timely treatment at the onset of lesion in smokers.

Functional CT of the lung has been suggested to be a potential biomarker to detect early perfusion abnormalities

by reflecting contrast material within the pulmonary vasculature. Moreover, dual-energy CT (DECT) angiography, based on their energetic absorption spectra to distinguish materials (8,9), enables the evaluation of lung morphology and parenchymal iodine distribution simultaneously without subjecting the patient to excessive radiation exposure. With the quantification of iodine density (ID), DECT may demonstrate the regional perfusion status of normal and abnormal structures. Existing investigations have reported on the viability of applying DECT for pulmonary embolism (PE) detection (10-12). According to a recent research by Weidman *et al.* (13), DECT iodine maps reveal an additional improvement for the identification of occlusive segmental and subsegmental PE. In recent years, spectral dual-layer detector CT (DLCT) has been introduced. This instrument acquires both conventional images and dual-energy images, allowing for the visualization and quantification of iodine maps, which can serve as a measurement for organ perfusion (14). We hypothesize that smoking may have an adverse effect on pulmonary perfusion in comparison to healthy control group, which might be revealed by spectral DLCT.

The purpose of this study was to investigate if there are additional values with iodine maps from spectral DLCT in assessing lung perfusion impairment of smokers. We present this article in accordance with the STROBE reporting checklist (available at <https://jtd.amegroups.com/article/view/10.21037/jtd-23-891/rc>).

Highlight box

Key findings

- The iodine map derived from spectral dual-layer detector computed tomography (DLCT) showed higher sensitivity in evaluating the pulmonary abnormalities of smokers compared with emphysema.

What is known and what is new?

- Abnormal pulmonary blood circulation is one of the most major pathophysiological alterations in smokers.
- Spectral DLCT acquires both conventional images and dual-energy images, allowing for the visualization and quantification of iodine maps.

What is the implication, and what should change now?

- Smoking may have an adverse effect on pulmonary perfusion in comparison to healthy population, which might be revealed by spectral DLCT, and targeting vascular therapy seems to be a promising treatment to cure and prevent disease progression. Therefore, assessment of the lung perfusion abnormality is very significant to timely treatment at the onset of lesion in smokers.

Methods

Study population

A total of 95 consecutive patients admitted to the department of respiration medicine in our hospital were recruited from June 2022 to September 2022 in this retrospective study. Twenty-one patients were excluded due to the lack of pulmonary function tests (PFTs). Nineteen patients were excluded because contrast enhanced spectral DLCT scan were not acquired at the admission. Patients with chest surgery, bilateral pleural effusion, history of diseases that might cause perfusion abnormalities such as pulmonary vaso-occlusive disease, obliterative bronchiolitis and hypersensitivity pneumonitis, obviously anomalous lung lesions on a CT scan or with radiographic features of lung infiltration, and cardiac or renal diseases were excluded. Two patients were excluded because of thoracic surgery. Five patients were excluded because of mild or moderate

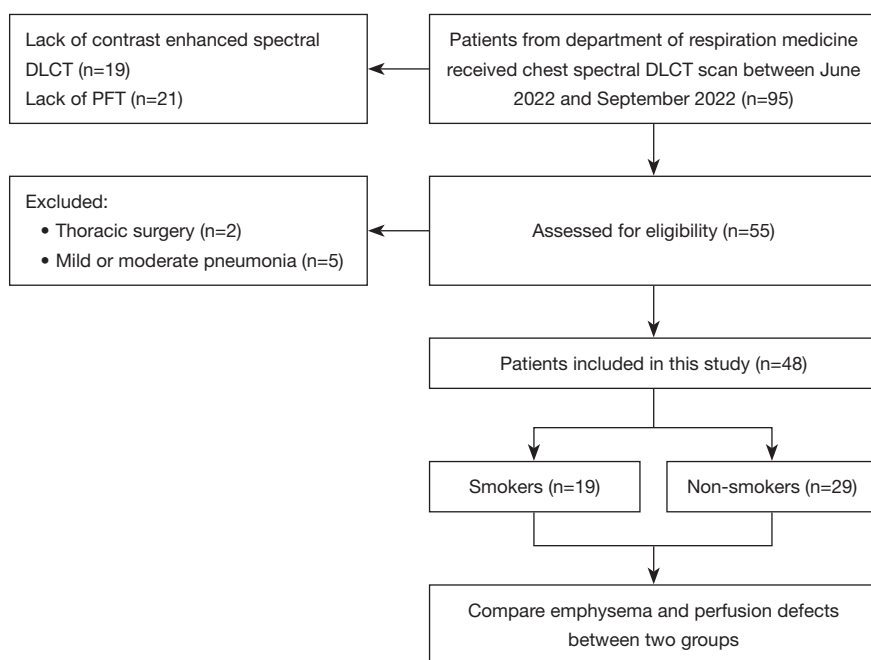


Figure 1 Flow diagram of the study. DLCT, dual-layer detector computed tomography; PFT, pulmonary function test.

pneumonia. Finally, 48 patients were included (*Figure 1*). The clinical symptoms including productive cough, breathlessness and wheezing were recorded according to the patients' complaints. The study was conducted in accordance with the Declaration of Helsinki (as revised in 2013). The study was approved by the ethics board of Changzheng Hospital, Naval Medical University, Shanghai, China (Approval No. PD_CT_Hawk_2021_11258) and individual consent for this retrospective analysis was waived.

The smoking history was documented and quantified in "pack-years", which were calculated by multiplying the number of packs smoked per day by the number of years the person had smoked. Smokers were defined as patients who smoked actively and had a total of or more than one month of smoking experience. Non-smokers were defined as patients who had never smoked or had smoked for less than one month (15). According to the definitions, the patients were divided into two subgroups: smokers and non-smokers. Of the 48 patients recruited in the study, 19 smokers and 29 non-smokers were included.

PFT

According to the official clinical practice guideline of the American Thoracic Society (16), the spirometer (Master

Screen Body; Hoechberg, Germany) was used to perform a PFT. The percentage of forced expiratory volume in 1 second (FEV_1) to the predicted value ($FEV_1\%$) and the ratio of FEV_1 to forced vital capacity (FVC) of all patients were recorded. The interval time between PFT and dual-phase contrast enhanced scan on spectral DLCT ranged from 0 to 5 days (median, 2 days).

Spectral DLCT scanning protocol

All patients in this retrospective study underwent dual-phase contrast enhanced scans of the chest on a spectral DLCT (Spectral 7500, Philips Healthcare, Best, The Netherlands). A craniocaudal spectral DLCT scan was carried out with the patient lying supine and both arms raised. Before each examination, holding breath training was performed. All patients were instructed to hold their breath as long as possible at the end of maximum inspiration. Dual-phase contrast enhanced scan was performed subsequent to non-contrast scan.

A body weight-based bolus of iodinated contrast medium (Accupaque, 350 mg/mL; GE Healthcare GmbH, Solingen, Germany) was administered into elbow vein at a speed of 3.5 mL/s followed by 30-mL saline solution at the same rate. The administered iodinated contrast agent volume

was based on patient body weight (kg) as 1.0 mL/kg. The range of weight was 54–76 kg (mean weight 68.92 ± 5.80 kg). Therefore, totally 18–26 g of iodine was used in our study. The arterial phase and venous phase acquisitions were performed at 28 and 65 s, respectively. The acquisition parameters are as follows: matrix, 512×512 ; collimation, 128×0.625 mm; pitch, 1.0; rotation time, 0.5 s; enabled tube current modulation (DoseRight 3D-DOM; Philips Healthcare) and tube voltage, 120 kVp. Non-enhanced images, and ID images from arterial phase of spectral data were reconstructed with 1 mm section thickness using standard kernel at 1 mm section increment.

Image quality evaluation and radiation dose

Two thoracic radiologists (with 8 and 10 years of experience, respectively) independently assessed ID images for each spectral DLCT examination on the Philips workstation (Extended Brilliance Workspace TM, Cleveland, OH, USA) based on the method of Singh *et al.* (17). They performed qualitative assessment of overall diagnostic quality based on the existence and severity of artifacts. Image quality was graded on 3-point scale (1= no artifacts; 2= minimal artifacts with no effect on diagnostic interpretation; 3= artifacts with substantial effect on diagnostic confidence, diagnosis not possible). The artifact types including cardiac motion artifacts, contrast streaking, beam hardening, metallic implant related artifacts were evaluated as well.

CT dose index volume (CTDIvol), size-specific dose estimates (SSDEs), and dose length product (DLP) were recorded for each patient.

Emphysema assessment on non-enhanced images

Qualitative analysis of emphysema: non-enhanced images were assessed at a window level of –450 Hounsfield units (HU) and a window width of 1,500 HU. Emphysema was scored visually at bilateral lung fields of three anatomic levels (total six lung fields) using the method of Goddard *et al.* (18). The three anatomic levels were the level of the superior margin of the aortic arch, the level of close to the carina, and the level of near the entrance of the inferior pulmonary veins, respectively. The emphysema was scored in each field at each level according to the following criteria: point 0, the lung had no lucency area; point 1, the lucency scope comprised 1–25%; point 2, the lucency scope comprised 26–50%; point 3, the lucency scope comprised 51–75%; point 3, the lucency scope comprised 76–100%;

the total score for bilateral lung fields at all three levels was calculated.

Quantitative analysis of emphysema: non-enhanced images data were analyzed by Philips workstation (Extended Brilliance Workspace TM). Emphysema was considered to be the lung attenuation below –950 HU in the lung parenchyma. Emphysema index (EI) was recorded as the volume percentage of the emphysematous lung at whole lung level.

Perfusion defect (PD) assessment on iodine maps

Qualitative analysis of PD: iodine maps at arterial phase image were reconstructed. PD was scored visually according to the above evaluation method of emphysema. The details are as follows: PD was scored visually in bilateral upper (at the level of superior margin of the aortic arch), middle (near the carina), and lower lung (close to the orifice of the inferior pulmonary veins) fields. The scores were calculated based on the ratio of the extent of PD occupied in the pulmonary field of each slice as described below: point 0, the lung presented homogeneous perfusion and had no PD; point 1, $0\% < \text{PD scope} \leq 25\%$; points 2, $25\% < \text{PD scope} \leq 50\%$; points 3, $50\% < \text{PD scope} \leq 75\%$; points 4, $\text{PD scope} > 75\%$. The sum of scores at bilateral lung fields at three levels for each patient was calculated. Then, the pattern of PDs was analyzed at three levels. Three types of PDs were assessed: (I) patchy defects; (II) triangular defects; (III) circumscribed, but not triangular defects.

Quantitative analysis of PD: iodine maps at arterial phase image were reconstructed. If PDs were present, regions of interest (ROIs) were measured on PDs and thoracic aorta on the slice of bilateral upper, middle, and lower pulmonary fields, respectively. and all the ROIs were noted to avoid the apparent pulmonary vascular structure and the area between $50\text{--}55 \text{ mm}^2$. The mean ID of the PDs and thoracic aorta was calculated as $\text{ID}_{\text{defect}}$ and $\text{ID}_{\text{thoracic aorta}}$. Then the ratio was calculated as the normalized ID (nID) ($\text{nID} = \text{ID}_{\text{defect}} / \text{ID}_{\text{thoracic aorta}}$).

All the qualitative and quantitative analyses of emphysema and PDs were interpreted independently by thoracic radiologists with 8 to 10 years of experience, and the ultimate results were determined based on the mean values of their analysis. The participants' identities and medical records were concealed from the observers. Due to the absence of electrocardiograph (ECG) gating, cardiac motion artifacts would potentially influence the findings of PDs occasionally. The two radiologists reached a consensus

Table 1 Clinical and demographic characteristics of the patients

Characteristics	Smokers (n=19)	Non-smokers (n=29)	P value
Sex (F/M)	6/13	12/17	0.493
Age (years)	61.7±8.25	59.95±8.72	0.78
BMI (kg/m ²)	24.33±0.88	25.04±0.91	0.051
Smoking (pack-years)	20 (17.5–40)	–	–
FEV ₁ % predicted value	89.22±20.85	99.15±15.06	0.166
FEV ₁ /FVC	76.59±8.44	81.39±8.11	0.144

Data are presented as n, mean ± standard deviation or median (interquartile range). F, female; M, male; BMI, body mass index; FEV₁, forced expiratory volume in 1 second; FVC, forced vital capacity.

to rule out pseudo-defects caused by pulsation artifacts or beam-hardening artifacts in the paracardiac pulmonary parenchyma.

Statistical analysis

All data were statistically analyzed using a SPSS 26.0 software (IBM SPSS Statistics, Armonk, NY, USA). Clinical, demographic characteristics and parameters of PD and emphysema were compared between smokers and non-smokers by using Student's *t*-tests and one-way analysis of variance (ANOVA) for normally distributed values and using Mann-Whitney *U*-tests for non-normally distributed data. Correlations between all measured data and PFT parameters were evaluated by Spearman correlation analysis. The measurement agreement of the two radiologists was evaluated by using intraclass correlation (ICC) coefficients. ICC was defined as very good (ICC >0.8), good (0.6 < ICC ≤ 0.8), moderate (0.4 < ICC ≤ 0.6), poor (ICC ≤ 0.4). All reported P values were two-sided with a 0.05 significance level.

Results

Patient population

A total of 48 spectral DLCT examinations were performed with good image quality. For all patients, the mean age was 60.75±8.43 years (median, 59 years; range, 43–80 years); for men, the mean age was 61.04±7.65 years (median, 59 years; range, 48–80 years); and for women, the mean age was 60.37±9.61 years (range, 43–75 years) (P=0.81). No differences in FEV₁% and FEV₁/FVC of smokers compared with non-smokers were observed (P=0.166; P=0.144). *Table 1*

shows the clinical and demographic features of the patients.

Image quality evaluation and radiation dose

Both radiologists reported minimal artifacts in 19/29 (65.5%) examinations of non-smokers and 13/19 (68.4%) examinations of smokers ($\chi^2=0.044$, P=0.835). No artifacts were reported in the remaining 10/29 (34.5%) exams examinations and 6/19 (31.6%) examinations in non-smokers group and smoker group, respectively ($\chi^2=0.044$, P=0.835). None of the severe artifacts resulted in diagnosis not possible. Artifacts included contrast streaking from subclavian veins, cardiac pulsation artifacts, and beam hardening at the level of the shoulders. And all the artifacts were categorized as minimal. Image quality was deemed good to meet the diagnosis for all examinations.

The CTDIvol, SSDE and DLP were 10.61±5.24 mGy, 15.54±4.84 mGy, 402.24±87.27 mGy*cm, respectively.

Emphysema findings on non-enhanced images

Five smokers and eight non-smokers manifested trace or mild emphysema visually, while 14 smokers and 21 non-smokers presented negative manifestations on non-enhanced CT images. No difference for emphysema positive rate was found between smokers and non-smokers (5/19 vs. 8/29; $\chi^2=0.009$, P=0.923). Meanwhile, there was no significant difference for emphysema visual scores between smokers and non-smokers (P=0.402). Although, EI increased slightly in tobacco smokers compared with non-smokers, no significant difference was observed between two groups (P=0.061) (*Table 2*). The ICC for emphysema visual scores between two measurements was very good for smokers (ICC, 0.9) and non-smokers (ICC, 0.86).

Table 2 Comparison of quantitative and qualitative analysis of emphysema and PDs between smokers and non-smokers

Variables	Smokers (n=19)	Non-smokers (n=29)	P value
Emphysema visual scores	1 [0–5.5]	1 [0–2.5]	0.402
EI (%)	4.30 [3.15–7.20]	2.10 [0.725–6.025]	0.061
PDs visual scores	7 [6–9]	6 [3.75–6]	0.014*
ID _{defect}	0.53 [0.38–0.69]	0.78 [0.59–1.14]	0.003*
nID	0.04 [0.03–0.06]	0.06 [0.04–0.07]	0.029*

Data are presented as median [interquartile range]. *, $P < 0.05$; PDs, perfusion defects; EI, emphysema index; ID_{defect}, iodine density of PD; nID, normalized iodine density.

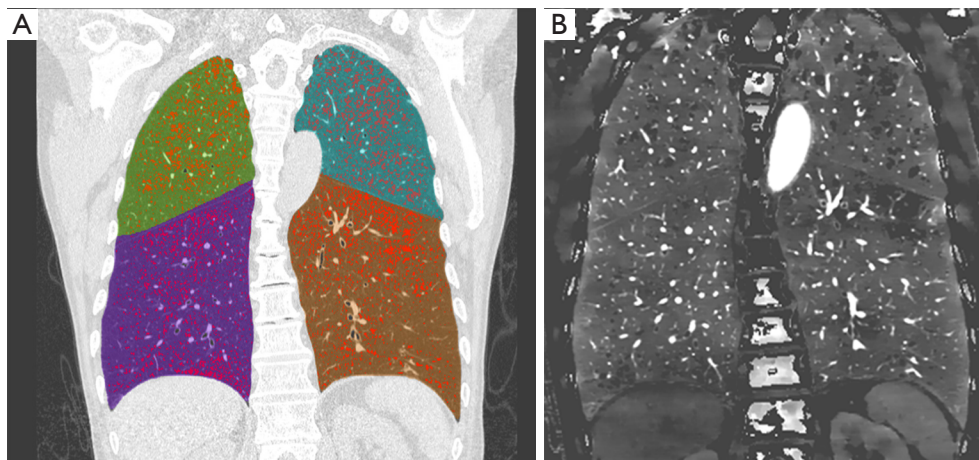


Figure 2 A 67-year-old man with smoking (18.6 pack-years). (A) Coronal CT image shows diffuse emphysema (red area) in the upper lobe (green) and lower lobe (purple) of right lung, the upper lobe (blue) and lower lobe (brown) of left lung. (B) Coronal iodine map image shows patchy PDs in corresponding level of lung. CT, computed tomography; PDs, perfusion defects.

Pulmonary perfusion findings on iodine map of arterial phase image

Varying degrees of PDs were observed in all smokers and the common pattern of PDs was the occurrence of patchy defects alone (Figure 2), triangular defects were just found in one smoker (Figure 3). Of the 29 non-smokers, 15 patients showed homogeneous perfusion on the ID images, and the other patients displayed with various degrees of PDs. In comparison to non-smokers, smokers had a higher positive rate of PDs observed on the ID images (19/19 vs. 14/29; $\chi^2 = 12.949$, $P < 0.001$). The PDs visual scores on ID images were significantly higher in smokers compared with that in non-smokers, while Both ID_{defect} and nID of PD were lower in smokers compared with non-smokers. There were significant differences for PDs visual scores and ID_{defect} and nID between smokers and non-smokers ($P = 0.014$; $P = 0.003$; $P = 0.029$)

(Table 2). For smokers, the ICC for PD visual scores was good (ICC, 0.8), the ICC for ID and nID were very good (ICC, 0.85; ICC, 0.90). In non-smokers, the ICC was very good for PD visual scores (ICC, 0.90), ID (ICC, 0.88) and nID (ICC, 0.95).

Correlations between PD on ID and emphysema and PFT parameters

Correlations of PFT parameters with emphysema and PD are shown in Table 3. In tobacco smokers, correlations of both emphysema visual scores and EI with FEV₁% or FEV₁/FVC were not observed. Yet, we found negative correlation between PDs visual scores and FEV₁% ($r = -0.61$, $P = 0.025$), or FEV₁/FVC ($r = -0.62$, $P = 0.024$). PDs visual scores increased with FEV₁% or FEV₁/FVC decreased. However, ID_{defect} and nID showed no correlation with FEV₁% or FEV₁/FVC (all $P > 0.05$). In non-smokers, EI was negatively correlated with

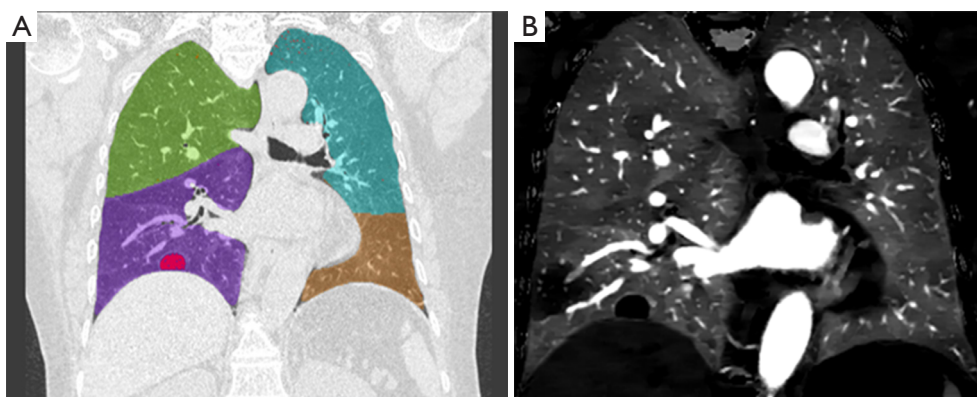


Figure 3 A 72-year-old woman with smoking (19.2 pack-years). (A) Coronal CT image shows pulmonary parenchyma without apparent emphysema. A bulla (red area) is seen in the lower lobe of the right lung (purple). The upper lobe of right lung (green). The upper lobe (blue) and the lower lobe (brown) of left lung. (B) Coronal iodine map image shows triangular PD in the lower lobe of right lung. There might be an embolus in the lower right pulmonary artery branch. And bulla present circumscribed but not triangular PD. CT, computed tomography; PD, perfusion defect.

Table 3 Correlations of PFT parameters with emphysema and PD

Variables	Smokers		Non-smokers	
	FEV ₁ %, r (P)	FEV ₁ /FVC, r (P)	FEV ₁ %, r (P)	FEV ₁ /FVC, r (P)
Emphysema visual scores	-0.43 (0.142)	-0.45 (0.125)	-0.29 (0.301)	0.14 (0.634)
EI	-0.22 (0.471)	-0.46 (0.112)	-0.62 (0.019)*	-0.31 (0.274)
PDs visual scores	-0.61 (0.025)*	-0.62 (0.024)*	-0.11 (0.708)	0.09 (0.761)
ID _{defect}	0.48 (0.094)	0.38 (0.194)	0.39 (0.159)	-0.13 (0.670)
nID	0.22 (0.471)	0.17 (0.578)	0.28 (0.326)	-0.04 (0.887)

The correlation coefficients r and P value are used to express the data. *, at the P<0.05 level, correlation is significant. PFT, pulmonary function test; PD, perfusion defect; FEV₁, forced expiratory volume in 1 second; FVC, forced vital capacity; EI, emphysema index; ID_{defect}, iodine density of PD; nID, normalized iodine density.

FEV₁% (r=-0.62, P=0.019), while correlation of emphysema visual scores with FEV₁% or FEV₁/FVC were not found (r=-0.29, P=0.301; r=0.14, P=0.634). In addition, there were no significant correlation between PDs visual scores, ID_{defect}, nID and FEV₁% or FEV₁/FVC for non-smokers (all P>0.05).

Discussion

The abnormalities of pulmonary perfusion could be qualitatively and quantitatively evaluated with the iodine map of DLCT (19). Inhomogeneous distribution of pulmonary perfusion was observed in the overall lung caused by smoking. Smokers had a greater positive detection rate of PDs on ID images than non-smokers. Patchy defects were the most

often observed for smokers. PD visual scores increased in tobacco smokers in comparison to non-smokers (P=0.014), and PDs visual scores increased with FEV₁% or FEV₁/FVC decreased (r=-0.61, P=0.025; r=-0.62, P=0.024) for smokers. ID and nID decreased in tobacco smokers compared with non-smokers (P=0.003; P=0.029). However, the similar results were not found for emphysema visual scores and EI.

Our findings suggest the presence of perfusion impairment in smokers, indicating the pulmonary vessels' abnormality caused by smoking, this result was consistent with the observations of Pansini *et al.* (20), who found that smokers with emphysema showed considerably lower attenuation enhancement values than smokers without emphysema. The frequently found patchy perfusion in smokers might

be attributed to two situations. First, the existence of emphysema indicates parenchymal destruction or without visually evaluated emphysematous changes on non-enhanced CT not precluding to underlying pulmonary destructive alterations. And local parenchymal destruction has been linked to corresponding pulmonary vascular reduction. Moreover, perfusion abnormalities of smokers might be associated with small microvascular remodelling produced by tobacco smoking, which has been discovered at an early stage of the disease. Contrary to what was expected, emphysema visual scores and EI did not differ between smokers and non-smokers in our investigation. The reason of this finding may be because that participants with smoking were more likely to be at an early stage of the pulmonary structural abnormality, and perfusion impairment in smokers may also be connected to pulmonary vascular dysfunction which often appears before alveolar destruction being detectable in smokers. Overall, our findings indicated that tobacco smoking had opposing effects on perfusion impairment as evaluated by spectral DLCT and we observed that local perfusion decreased without significant emphysema after tobacco consumption. This supported earlier research (21), demonstrating smoking leads to an imbalance between the destruction of lung parenchyma and perfusion impairment. Nyilas *et al.* (22) recently studied the short-term responsiveness of lung perfusion and ventilation after smoking by evaluating with a matrix pencil magnetic resonance imaging (MRI) and discovered that perfusion decreased after smoking exposure compared with the baseline measurement and no systematic change in fractional ventilation impairment. Other recent investigations have found that the microvascular endothelial cell is damaged for COPD patients and that the extent of impairment is related to the severity of airway limitation (23,24), similar to our results that PDs visual scores increased with FEV₁% or FEV₁/FVC decreased for smokers, indicating that PD visual scores could reflect the level of airway limitation. This finding was not confirmed by the ID and nID though. This could be attributable to the quantitative measurement of PD, which reflects local perfusion reduction or defect but not the whole lung perfusion impairment. Therefore, visual assessment of PD is more sensitive to suggest the change of lung function compared to quantitative measurement of PD. According to previous researches, the perfused blood volume (PBV) map of DECT has been shown to be comparable to conventional perfusion scintigraphy for evaluating pulmonary perfusion (25,26). PBV maps can be color-coded and imposed as a color fused overlay on the anatomical structure images to depict the enhancement of

the lung parenchyma at a particular time point computed from the iodine distribution in the pulmonary parenchyma from spectral data at low and high kVp. Fuld *et al.* (27) confirmed that visual analysis of the PBV color maps revealed that there was a significant relationship between DECT and dynamic multidetector CT for evaluating regional pulmonary parenchymal perfusion, and could be as surrogate for pulmonary perfusion. Meanwhile, the ID images of spectral detector CT (SDCT) are also considered as an effective intermediary parameter for assessing pulmonary perfusion. The research of Gertz *et al.* (28) showed that patients with PH had a considerably increased extent of decreased lung perfusion as well as more homogenous PDs by pulmonary perfusion maps of SDCT. Therefore, the capacity of spectral DLCT to evaluate iodine can be valuable for evaluating smoking-related pulmonary diseases.

We acknowledge that our investigation has several limitations. First, there was no attempt to match interpretations from this investigation to function MR perfusion, which has been confirmed with high sensitivity and accuracy by many clinical researches. Second, although earlier research linked iodine map abnormalities to pulmonary embolism, we did not have significant longtime follow-up for participants in our investigation to evaluate the clinical significance of perfusion impairments. Third, because our investigation was conducted at a single hospital, the sample size was quite limited. And smokers were not further divided into subgroups of current smokers or former smokers. At the same time, the perfusion impairments based on the varying smoking indices were not analyzed. To obtain more precise and persuasive findings, further multi-center trials including larger targeted populations of smokers with less emphysematous lung are required. Finally, the regular iodine amount existed in the contrast agent may have an influence to the results of the study. In future studies, we hope to further investigate lung perfusion changes of iodine maps with low iodinated contrast agent volume in smokers.

Conclusions

Compared with emphysema, the iodine map derived from spectral DLCT showed higher sensitivity for the evaluation of the pulmonary abnormalities of smokers.

Acknowledgments

Funding: This research was funded by the National

Natural Science Foundation Key Program of China (No. 81930049), the National Natural Science Foundation General Program of China (Nos. 82171926 and 81871321), the National Key Research and Development Program of China (Nos. 2022YFC2010002 and 2022YFC2010000), and the Changzheng Youth Science Support Program of China (No. CZQNKP-TYYX-LZ-2022-06).

Footnote

Reporting Checklist: The authors have completed the STROBE reporting checklist. Available at <https://jtd.amegroups.com/article/view/10.21037/jtd-23-891/rc>

Data Sharing Statement: Available at <https://jtd.amegroups.com/article/view/10.21037/jtd-23-891/dss>

Peer Review File: Available at <https://jtd.amegroups.com/article/view/10.21037/jtd-23-891/prf>

Conflicts of Interest: All authors have completed the ICMJE uniform disclosure form (available at <https://jtd.amegroups.com/article/view/10.21037/jtd-23-891/coif>). The authors have no conflicts of interest to declare.

Ethical Statement: The authors are accountable for all aspects of the work in ensuring that questions related to the accuracy or integrity of any part of the work are appropriately investigated and resolved. The study was conducted in accordance with the Declaration of Helsinki (as revised in 2013). The study was approved by the ethics board of Changzheng Hospital, Naval Medical University, Shanghai, China (Approval No. PD_CT_Hawk_2021_11258) and individual consent for this retrospective analysis was waived.

Open Access Statement: This is an Open Access article distributed in accordance with the Creative Commons Attribution-NonCommercial-NoDerivs 4.0 International License (CC BY-NC-ND 4.0), which permits the non-commercial replication and distribution of the article with the strict proviso that no changes or edits are made and the original work is properly cited (including links to both the formal publication through the relevant DOI and the license). See: <https://creativecommons.org/licenses/by-nc-nd/4.0/>.

References

1. Rennard SI, Vestbo J. COPD: the dangerous underestimate of 15%. *Lancet* 2006;367:1216-9.
2. Woodruff PG, Barr RG, Bleecker E, et al. Clinical Significance of Symptoms in Smokers with Preserved Pulmonary Function. *N Engl J Med* 2016;374:1811-21.
3. Regan EA, Lynch DA, Curran-Everett D, et al. Clinical and Radiologic Disease in Smokers With Normal Spirometry. *JAMA Intern Med* 2015;175:1539-49.
4. Park J, Hobbs BD, Crapo JD, et al. Subtyping COPD by Using Visual and Quantitative CT Imaging Features. *Chest* 2020;157:47-60.
5. Wang M, Aaron CP, Madrigano J, et al. Association Between Long-term Exposure to Ambient Air Pollution and Change in Quantitatively Assessed Emphysema and Lung Function. *JAMA* 2019;322:546-56.
6. Ferrer E, Peinado VI, Castañeda J, et al. Effects of cigarette smoke and hypoxia on pulmonary circulation in the guinea pig. *Eur Respir J* 2011;38:617-27.
7. Seimetz M, Parajuli N, Pichl A, et al. Inducible NOS inhibition reverses tobacco-smoke-induced emphysema and pulmonary hypertension in mice. *Cell* 2011;147:293-305.
8. Geyer LL, Scherr M, Körner M, et al. Imaging of acute pulmonary embolism using a dual energy CT system with rapid kVp switching: initial results. *Eur J Radiol* 2012;81:3711-8.
9. Bauer RW, Kramer S, Renker M, et al. Dose and image quality at CT pulmonary angiography-comparison of first and second generation dual-energy CT and 64-slice CT. *Eur Radiol* 2011;21:2139-47.
10. Vlahos I, Jacobsen MC, Godoy MC, et al. Dual-energy CT in pulmonary vascular disease. *Br J Radiol* 2022;95:20210699.
11. Hong YJ, Shim J, Lee SM, et al. Dual-Energy CT for Pulmonary Embolism: Current and Evolving Clinical Applications. *Korean J Radiol* 2021;22:1555-68.
12. Abozeed M, Conic S, Bullen J, et al. Dual energy CT based scoring in chronic thromboembolic pulmonary hypertension and correlation with clinical and hemodynamic parameters: a retrospective cross-sectional study. *Cardiovasc Diagn Ther* 2022;12:305-13.
13. Weidman EK, Plodkowski AJ, Halpenny DE, et al. Dual-Energy CT Angiography for Detection of Pulmonary Emboli: Incremental Benefit of Iodine Maps. *Radiology* 2018;289:546-53.

14. Mochizuki J, Nakaura T, Yoshida N, et al. Spectral imaging with dual-layer spectral detector computed tomography for the detection of perfusion defects in acute coronary syndrome. *Heart Vessels* 2022;37:1115-24.
15. Yu N, Yuan H, Duan HF, et al. Determination of vascular alteration in smokers by quantitative computed tomography measurements. *Medicine (Baltimore)* 2019;98:e14438.
16. Miller MR, Hankinson J, Brusasco V, et al. Standardisation of spirometry. *Eur Respir J* 2005;26:319-38.
17. Singh R, Sharma A, McDermott S, et al. Comparison of image quality and radiation doses between rapid kV-switching and dual-source DECT techniques in the chest. *Eur J Radiol* 2019;119:108639.
18. Goddard PR, Nicholson EM, Laszlo G, et al. Computed tomography in pulmonary emphysema. *Clin Radiol* 1982;33:379-87.
19. Gietema HA, Walraven KHM, Posthuma R, et al. Dual-Energy Computed Tomography Compared to Lung Perfusion Scintigraphy to Assess Pulmonary Perfusion in Patients Screened for Endoscopic Lung Volume Reduction. *Respiration* 2021;100:1186-95.
20. Pansini V, Remy-Jardin M, Faivre JB, et al. Assessment of lobar perfusion in smokers according to the presence and severity of emphysema: preliminary experience with dual-energy CT angiography. *Eur Radiol* 2009;19:2834-43.
21. Rieben FW. Acute ventilation-perfusion mismatching resulting from inhalative smoking of the first cigarette in the morning. *Clin Investig* 1992;70:328-34.
22. Nyilas S, Bauman G, Korten I, et al. MRI Shows Lung Perfusion Changes after Vaping and Smoking. *Radiology* 2022;304:195-204.
23. Harris B, Klein R, Jerosch-Herold M, et al. The association of systemic microvascular changes with lung function and lung density: a cross-sectional study. *PLoS One* 2012;7:e50224.
24. Kyomoto Y, Kanazawa H, Tochino Y, et al. Possible role of airway microvascular permeability on airway obstruction in patients with chronic obstructive pulmonary disease. *Respir Med* 2019;146:137-41.
25. Chae EJ, Kim N, Seo JB, et al. Prediction of postoperative lung function in patients undergoing lung resection: dual-energy perfusion computed tomography versus perfusion scintigraphy. *Invest Radiol* 2013;48:622-7.
26. Thieme SF, Becker CR, Hacker M, et al. Dual energy CT for the assessment of lung perfusion--correlation to scintigraphy. *Eur J Radiol* 2008;68:369-74.
27. Fuld MK, Halaweish AF, Haynes SE, et al. Pulmonary perfused blood volume with dual-energy CT as surrogate for pulmonary perfusion assessed with dynamic multidetector CT. *Radiology* 2013;267:747-56.
28. Gertz RJ, Gerhardt F, Kröger JR, et al. Spectral Detector CT-Derived Pulmonary Perfusion Maps and Pulmonary Parenchyma Characteristics for the Semiautomated Classification of Pulmonary Hypertension. *Front Cardiovasc Med* 2022;9:835732.

Cite this article as: Guan Y, Zhou X, Zhang D, Xia Y, Liu S, Fan L. The characteristics of emphysema and pulmonary perfusion derived from spectral CT in smokers. *J Thorac Dis* 2023;15(11):6084-6093. doi: 10.21037/jtd-23-891